# Supplemental Material

## Online Supplemental Methods

All procedures involving the handling of animals were approved by the Animal Care and Use Committee of the Johns Hopkins University and adhered to National Institutes of Health guidelines.

**Labeling of Sarcolemma and RyRs**. The sarcolemma was labeled using wheat germ agglutinin (WGA) conjugated to Alexa Fluo-555 (Molecular Probes, Eugene, OR) as described previously.[1] The cells were fixed for 10 min at room temperature with 1% paraformaldehyde and washed afterwards with phosphate buffered saline (PBS) solution. Cells were attached to a chamber using polylysine and permeabilized with PBS solution containing 0.3% Triton X-100 for 15 min. After washing with PBS cells were bathed in Image-iT FX Signal Enhancer (Molecular Probes, Eugene, OR) for 30 min. Subsequently, cells were washed and blocked for 60 min using a PBS solution containing 10% normal goat serum (NGS, Millipore, Billerica, MA) and 0.05% Triton X-100. Afterwards the cells were incubated overnight at 4°C with the monoclonal anti-RyR2 antibody (C3-33) (Pierce Biotechnology, Rockford, IL) prepared in PBS-incubation solution containing 2% bovine serum albumin (BSA), 2% NGS and 0.05 % Triton X-100. The cells were washed with PBS and incubated for 60 min with a secondary goat anti mouse IgG (H+L) antibody attached to Alexa Fluor 488 (Molecular Probes, Eugene, OR). The next day the cells were washed and stored in PBS solution. ProLong Gold Antifade Reagent (Molecular Probes, Eugene, OR) was added to the cells 24 h prior to imaging.

**Imaging Protocol.** The confocal aperture was set to an Airy number of 1. Alexa Fluor 488 was excited with a 488 nm laser line and the emitted light was band-pass filtered at 505 to 530 nm. Alexa Fluor 555 was excited with a 543 nm laser and the emitted light long-pass filtered at 560 nm. A two-track protocol was used to provide for spatial registration of the WGA and RyR image stacks. With this protocol the imaging of WGA and RyR associated fluorescence was performed quasi-simultaneously by alternating WGA and RyR imaging for each image of the 3D stack. Using this imaging protocol the separation of excitation and emission spectra of the applied fluorophores assures that cross-talk between WGA and RyR signals is negligible. Image stacks covered transversal segments of myocytes with a typical dimension of 512 (width) x 128 (length) x 200 (height) voxels at a resolution of 100 nm in the x, y and z direction. Imaging of a cell segment required ~30 min. After acquisition of an image stack a single image at half height was taken and visually compared to images in the stack. Image stacks were rejected if the visual inspection revealed that the image was shifted more than 5% of the height of the image stack. Visual inspection was also carried out to reject image stacks with insufficient WGA or RyR intensity and imaging artefacts, such as vibration and drift.

**Image Processing and Deconvolution.** The methodology for processing of confocal microscopic images has been described previously.[1-4] The software was implemented in C++, Perl and Matlab 7.9 (The Mathworks, Inc., Natick, MA). In short, we applied methods for noise reduction, removal of background signals, correction of depth-dependent attenuation, and deconvolution. Deconvolution of the image stacks was based on the Richardson-Lucy algorithm[5,6] with measured point spread functions (PSFs). The PSFs were obtained from images of fluorescent beads (diameter: 100 nm; excitation wave length: 505 nm; emission wavelength: 515 nm) (Molecular Probes, Eugene, OR) suspended in 0.2% agarose. The PSFs (number of PSFs: 6) were aligned and averaged. The averaged PSF exhibited a full width at half maximum (FWHM) of ~260 nm in xy and ~750 nm in z direction. Measured PSFs in regions above 20 µm of the glass slide exhibited a small signal-to-noise ratio and were not used in this process. Based on this finding, we also restricted further processing of the image data to regions within 12 µm of the glass slide.

**Frequency Analysis of T-System and RyR distribution.** Spatial distributions of the t-system and RyR distribution in the image stacks were characterized from their Fourier spectra.[7] Fourier analyses have been established previously for characterizing alignment and arrangement of structures and tissues.[8-10] A discrete three-dimensional Fourier transform was applied on the image data after multiplying them with a Gaussian window function. The width of the Gaussian window was set to attenuate signals for regions with outer sarcolemma. Intensities in spherical sectors with a central angle of 10º at spatial frequencies from 0.4 to 2 $\mu m^{-1}$ and 0.4 and 1 $\mu m^{-1}$ were integrated from the t-system and RyR spectra, respectively. Sectioning of a two-dimensional Fourier domain is illustrated in Online Figure III. As a measure of directionality of structures served the ratio of summed intensities within 12.5º to the (0,1,0) axis in the frequency domain to the overall sum of intensities in the spherical sectors.

## Online Tables

| | LVEDP [mmHg] | LVESP [mmHg] | $dP/dt_{max}$ [mmHg/s] | $dP/dt_{min}$ [mmHg/s] | Sinus HR [$min^{-1}$] |
|---|---|---|---|---|---|
| Control | 7.1±4.3 | 135.5±24.2 | 1980.2±229.2 | -2220.8±425.7 | 122.0±25.3 |
| A6 | 27.7±14.0 | 122.3±13.0 | 1178.2±318.8 | -1339.2±281.7 | 147.5±17.2 |
| DHF | 21.1±7.3 | 91.6±21.0 | 802.9±252.3 | -1039.8±239.0 | 128.9±18.1 |
| CRT | 28.2±13.3 | 106.1±19.1 | 1024.1±213.9 | -1256.8±214.8 | 164.8±14.2 |

**Online Table I: Hemodynamics parameters (mean±stddev).** LVEDP, LV end-diastolic pressure; LVESP, LV end-systolic pressure; and HR, heart rate.

| | Anterior [Cells/animals] | Lateral [Cells/animals] |
|---|---|---|
| Control | 24/6 | 26/10 |
| A6 | 24/8 | 22/8 |
| DHF | 20/7 | 21/7 |
| CRT | 32/10 | 25/9 |

**Online Table II: Numbers of cells and animals for structural studies.**

## Online Figures

Online Figure I

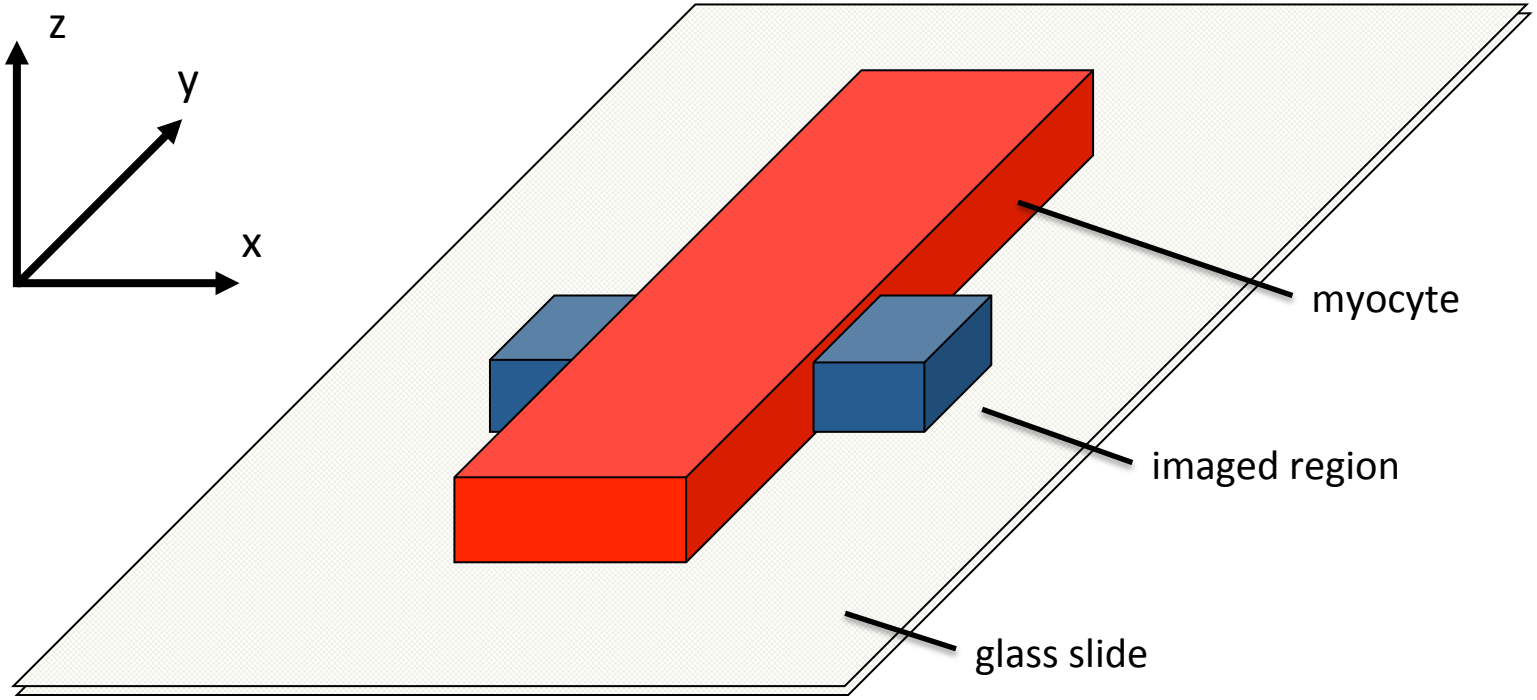


**Online Figure I. Configuration for confocal microscopic imaging of myocytes.** The imaged region covers a myocyte segment with a typical size of 51.2 µm x 12.8 µm x 20 µm (width x length x height). The y-axis in the image stacks is parallel to the long axis of the cell. The x-axis is orthogonal in the horizontal imaging plane. The z-axis is parallel to the laser direction.

Online Figure II

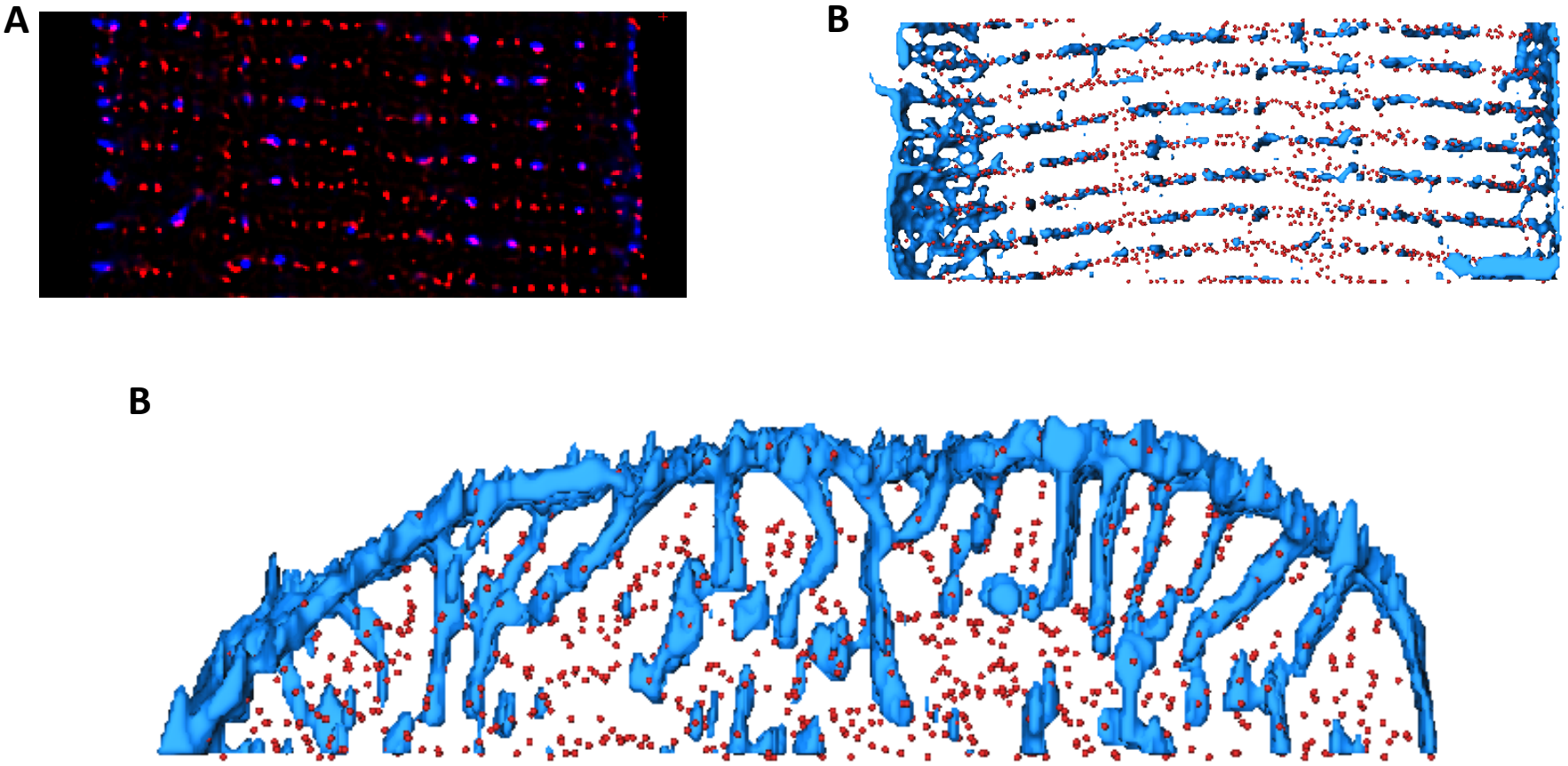


**Online Figure II. Images and reconstruction of of segment from anterior myocytes of normal canine. A**, Deconvolved confocal microscopic image of WGA (blue) and RyR (red) labeling. Three-dimensional reconstruction of WGA distribution and centers of RyR clusters (**B,** longitudinal section viewed along z-axis, **C,** transverse section viewed along y-axis).

Online Figure III

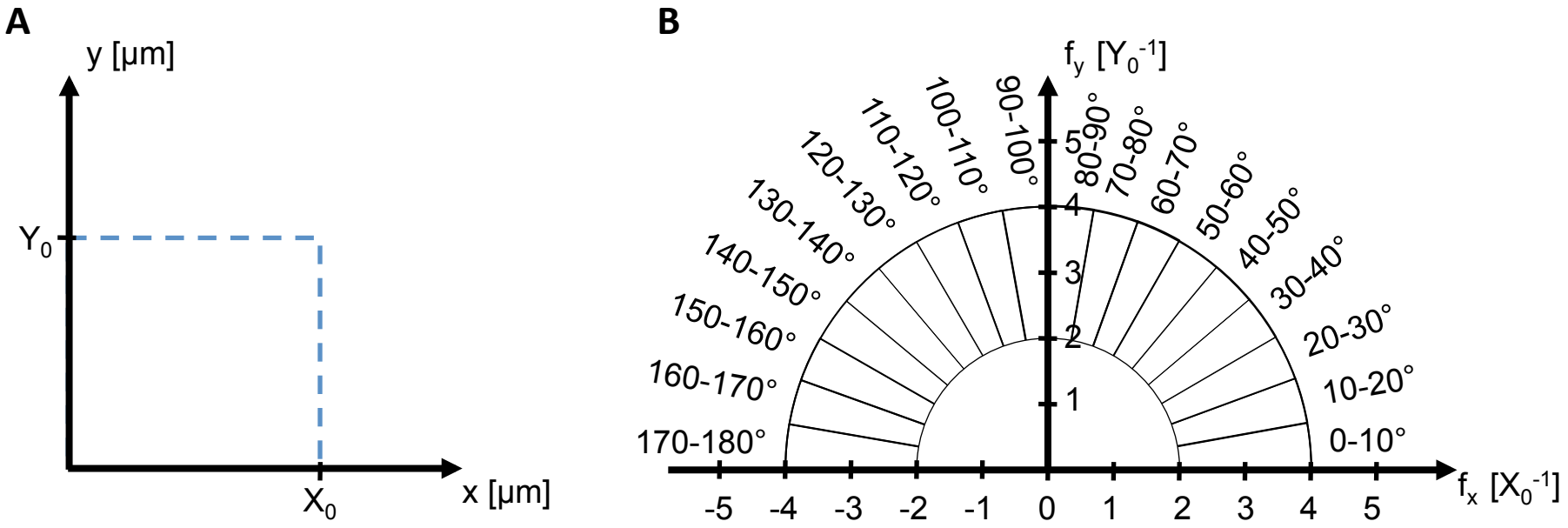


**Online Figure III. A, Spatial domain and B, sectioning in two-dimensional Fourier domain.** The opening angle of each sector is $10^o$. Sectors span from spatial frequencies of 2 to 4. Only a half spectrum is shown due to symmetry.

Online Figure IV

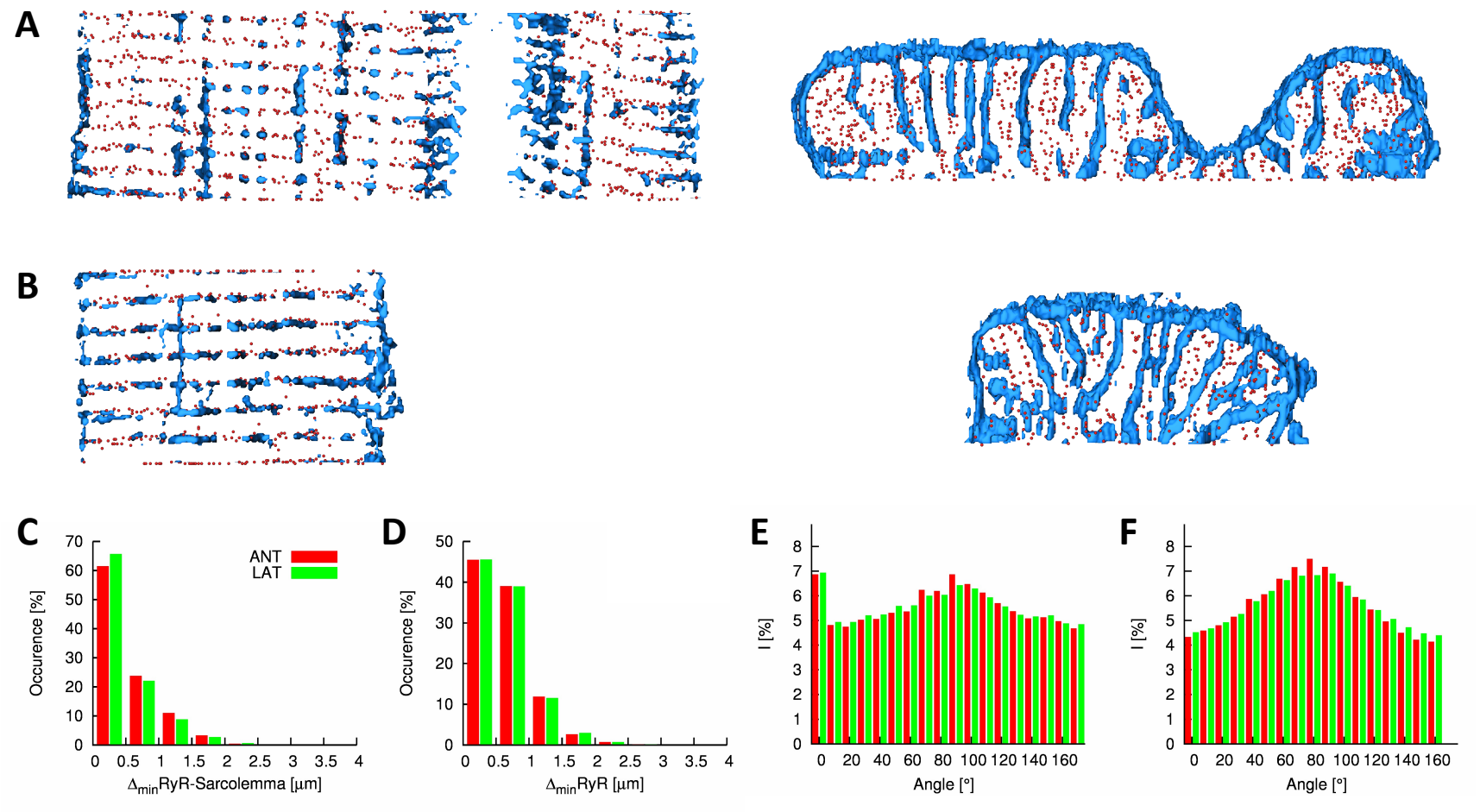


**Online Figure IV. Images and reconstruction of of segment from A, anterior and B, lateral myocytes of A6 canine.** Three-dimensional reconstruction of WGA distribution (blue) and centers of RyR clusters (red). Histogram of **C**, distances between RyR clusters and the closest sarcolemma and **D**, distances of RyR clusters to their nearest neighbor. Fourier intensities of **E**, WGA and **F**, RyR labeled image stacks.

## Supplemental References


**1.** Sachse FB, Savio-Galimberti E, Goldhaber JI, Bridge JH. Towards computational modeling of excitation-contraction coupling in cardiac myocytes: reconstruction of structures and proteins from confocal imaging. *Pacific Symposium on Biocomputing.* 2009:328-339.

**2.** Savio E, Goldhaber JI, Bridge JHB, Sachse FB. A framework for analyzing confocal images of transversal tubules in cardiomyocytes. *Lect Notes Comput Sci.* 2007;4466:110-119.

**3.** Savio-Galimberti E, Frank J, Inoue M, et al. Novel features of the rabbit transverse tubular system revealed by quantitative analysis of three-dimensional reconstructions from confocal images. *Biophys J.* 2008.

**4.** Lasher RA, Hitchcock RW, Sachse FB. Towards Modeling of Cardiac Micro-Structure With Catheter-Based Confocal Microscopy: A Novel Approach for Dye Delivery and Tissue Characterization. *IEEE T Med Imaging.* Aug 2009;28:1156- 1164.

**5.** Richardson WH. Bayesian-based iterative method of image restoration. *J. Opt. Soc. Am.* 00/1972 1972;62:55-59.

**6.** Lucy LB. An interative technique for the rectification of observed distributions. *Astronomical Journal.* 06/1974 1974;79:745.

**7.** Brigham EO. *The Fast Fourier Transform and Its Applications*: Prentice Hall; 1988.

**8.** Nichol JW, Engelmayr GC, Jr., Cheng M, Freed LE. Co-culture induces alignment in engineered cardiac constructs via MMP-2 expression. *Biochem Biophys Res Commun.* Aug 29 2008;373:360-365.

**9.** Engelmayr GC, Jr., Cheng M, Bettinger CJ, Borenstein JT, Langer R, Freed LE. Accordion-like honeycombs for tissue engineering of cardiac anisotropy. *Nat Mater.* Dec 2008;7:1003 -1010.

**10.** Ayres CE, Jha BS, Meredith H, et al. Measuring fiber alignment in electrospun scaffolds: a user's guide to the 2D fast Fourier transform approach. *J Biomater Sci Polym Ed.* 2008;19:603 -621.